# CRUSTAL DYNAMICS IN CALIFORNIA: IMPLICATIONS FOR LARGE-SCALE CSP TOWER SYSTEMS

Clement A. Ogaja, PhD
Assistant Professor, Department of Civil and Geomatics Engineering
California State University, Fresno
2320 East San Ramon Avenue M/S EE94,
Fresno, California 93740-8030, U.S.A.
E-Mail: cogaja@csufresno.edu

ABSTRACT

This paper presents a perspective for precise sunray reflection geometry in concentrating solar power (CSP) tower systems in the presence of crustal deformation. The CSP technology, based on a large field of small flat mirrors (heliostats) which track the sun with high precision, is an attractive renewable energy option in the southwestern United States and other sunbelts worldwide. In California, many areas are known to be continuously undergoing deformation due to plate boundary tectonics and human factors such as groundwater withdrawal. Dense GPS networks, InSAR technology and other instrumentation have provided meaningful long-term data to support these claims. Against this background, the paper looks at the potential role that crustal deformations might play in the long-term stability of such projects. Theoretical analyses indicate that relative crustal deformations of magnitudes as small as 0.06 m would potentially affect the dynamic angle by which the tracking mirror should rotate in order to stay on its target.

## 1. INTRODUCTION

New policies for clean energy technologies have resulted in what much of the media has termed as the 'Modern Day Cleantech Gold Rush'. In a report by LA Times (October 18, 2009), dozens of companies had flooded federal offices with applications to place solar mirrors on more than a million acres of public land across the desert flatlands of southeastern California. The technology is relatively new and untested in large scale but the potential to harness solar thermal power for clean electricity generation has been demonstrated. For instance, eSolar Inc, a California-based company, designs and develops Concentrating Solar Power (CSP) projects that start at 46MW and are scalable to any size—according to their website www.esolar.com (accessed on March 3, 2010). Their power plant technology utilizes small, flat mirrors which track the sun with high precision and reflect the sun's heat to a tower-mounted receiver, which boils water to create steam. This steam powers a traditional turbine and generator to produce solar electricity. The technology relies on precise sunray reflection from flat mirrors installed on a flatland such as those found in the deserts of California. However, California is known to be sitting on many active faults with the major one, San Andreas fault, running through much of its entire coastline. About 10,000 quakes each year rattle Southern California alone, although most of them are too small to be felt. Land subsidence is also a common occurrence due to groundwater withdrawal for economic activities such as farming and urban livelihood, and long-term studies from satellite-based GPS data have shown the Californian plate is constantly moving at rates of up to 50 mm/year.

In view of the above, this paper considers a methodology to assess the feasibility of potential long-term effects of relative crustal deformation on the precision of CSP sunray reflection given that such projects may have many years of design life. The existing geodetic infrastructure of space-based technologies such as InSAR and continuous GPS tracking stations can add to the benefit of such studies.

## 2. CONCENTRATED SOLAR POWER (CSP) TECHNOLOGY

With billions in government funding allocated globally, clean technology is now a leading venture investment sector, eclipsing biotech and IT. The leading clean technology sector is solar, which in the third quarter of 2008 alone, raised $1.2 billion in venture capital. Given the worldwide potential for solar harnessing (Fig. 1), several companies are looking at different viable alternatives for providing solar-generated power in large scale. This paper considers the CSP technology which uses mirrors and tracking systems to focus a large area of sunlight into concentrated light. The concentrated light is then used as a heat source for a conventional power plant. A wide range of

CSP technologies exist—including, for example, the parabolic trough, Concentrating Linear Fresnel Reflector, Solar chimney and solar power tower. The Sierra Sun Tower in Lancaster, Southern California (Fig. 2) and the Planta Solar 10 (PS10) in Sanlucar la Mayor, Spain are representative of the CSP technology using flat mirrors.

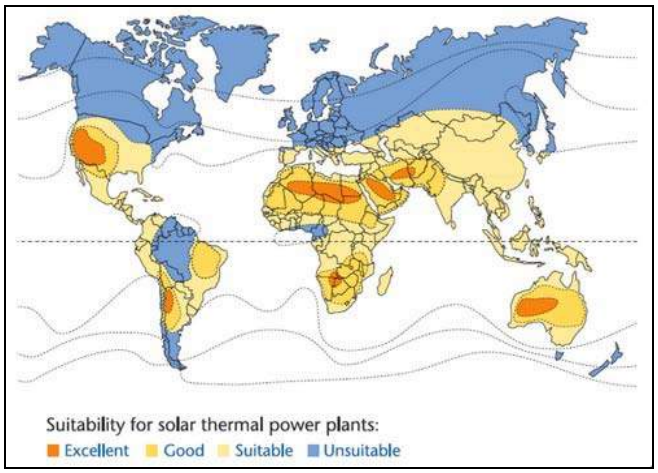

Fig. 1: Global suitability map for solar thermal power plants

Fig. 2: Sierra Sun Tower: eSolar demonstration solar farm outside the Southern California town of Lancaster (Photo Credit eSolar Inc.)

The Sierra Sun Tower, a demonstration solar farm outside the Southern California town of Lancaster, comprises of 24,000 mirrors called heliostats that surround two 150-foot towers (Fig. 2). The heliostats concentrate sunlight on a tower containing water-filled boilers and the resulting heat creates steam that drives an electricity-generating turbine.

The schematic in figure 3 illustrates how the CSP technology works. The steps include:

1. A field of sun-tracking heliostats reflects solar heat to a thermal receiver mounted atop a tower.
2. The focused heat boils water within the thermal receiver and produces steam.
3. The plant pipes the steam from each thermal receiver and aggregates it at the turbine.
4. The steam powers a standard turbine and generator to produce solar electricity.

The steam then reverts back to water through cooling, and the process repeats.

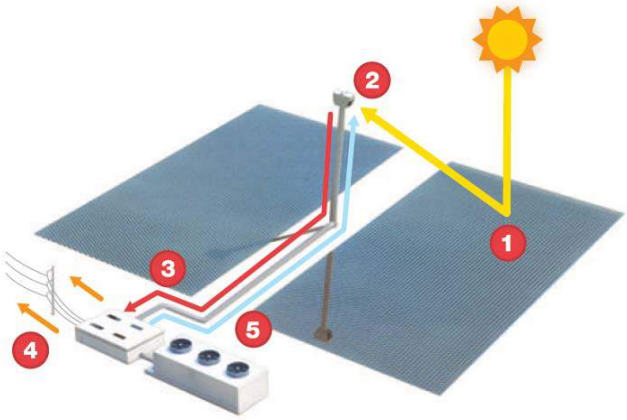

Fig. 3: How the CSP technology works (eSolar Inc.)

## 3. CRUSTAL DEFORMATION IN CALIFORNIA

### 3.1 Plate Tectonics and Deformation at Plate Boundaries

California is one of the most seismically active regions in the world. More than 300 faults crisscross the state, which sits atop two of the Earth's major tectonic plates, the Pacific and North American plates. San Andreas Fault system runs through all of the major cities of California including the San Francisco and LA basins. New calculations by USGS reveal there is a 99.7% chance a magnitude 6.7 quake or larger will hit the Golden State in the next 30 years. The odds of such an event are higher in Southern California than Northern California, 97% versus 93%. Long-term studies by dense GPS networks (Fig. 4, Hackl et al. 2009) and other techniques reveal active crustal movement around the San Andreas Fault system.

### 3.2 Human-Induced Deformation

In addition to the natural crustal deformation at plate boundaries, there is also land deformation caused by human factors. Past studies using conventional techniques, satellite-based GPS data, and other space technologies such as radar interferometry/InSAR and Satellite Gravity missions (GRACE and CHAMP) have shown evidence of regional

ground subsidence due to groundwater withdrawal and other activities such as geothermal exploration (see, e.g., Bertoldi et al. 1991; Ge at al 2009; and Watson et al. 2002).

In the present study, some case examples of human-induced deformation in California are shown in figures 5, 6 and 7. The first two are respectively InSAR images of ground displacement in Lancaster and Bakersfield areas, due to groundwater withdrawal. Similar studies with InSAR and GPS have shown human-induced deformation in the LA basin (USGS, 2005).

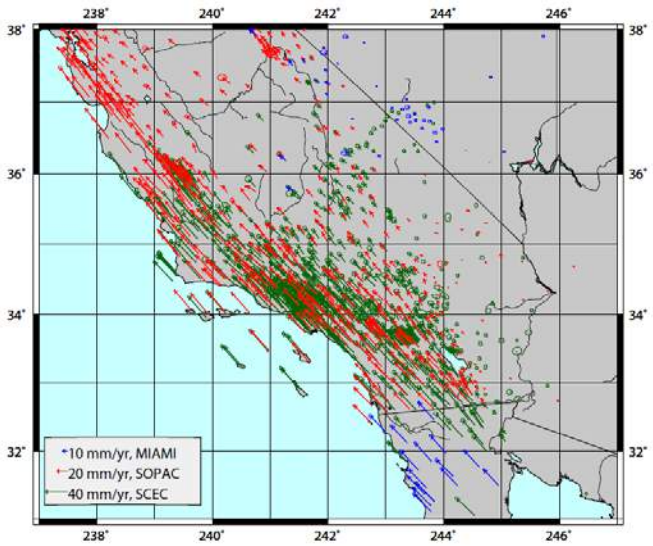


Fig. 4: Map of Southern California showing ground velocity arrows from dense GPS networks. Red arrows are velocities provided by the Scripps Orbit and Permanent Array Center (SOPAC); blue arrows are from University of Miami; green arrows are from crustal motion map by the Southern California Earthquake Center (SCEC) (Hackl et al. 2009)

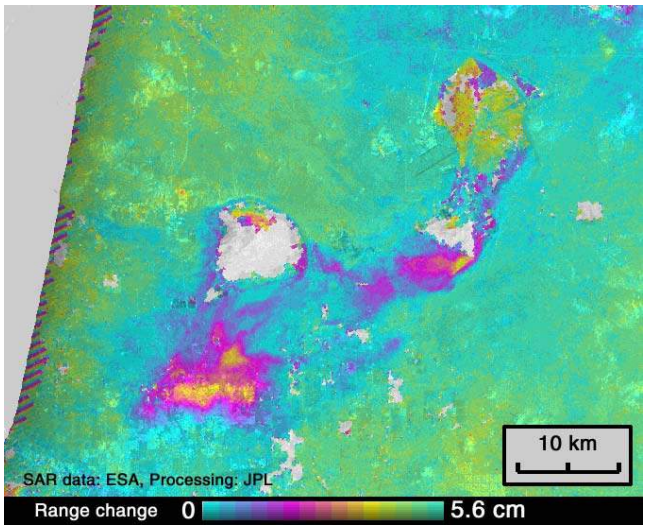


Fig. 5: Ground subsidence near Lancaster, California, April 28, 1993—October 13, 1995 (Source: JPL NASA)

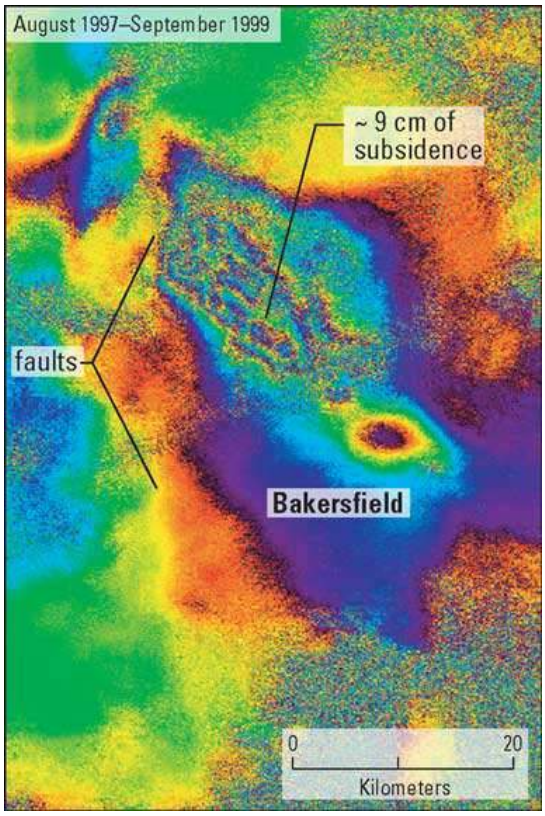


Fig. 6: Ground subsidence in Bakersfield, California, 1997—1999 (Source: USGS)

## 4. METHODOLOGY

Given that much of California is continuously deforming, what would be the impact of absolute or relative ground movements (if any) on the flat mirror technology for solar harnessing? In this section, an approach is developed to simulate the potential effects of relative deformation on the geometry of sunray reflection in a CSP project.

It is prudent to assume that crustal deformation will be problematic only if uneven deformation occurs at a CSP project site (Fig. 3). Horizontal deformation such as in figure 4 may be of no consequence unless the project is located on a fault line with different slippage rates. Similarly, homogeneous vertical deformations may not be a cause for concern. Assume further that any relative deformations at a CSP site can be accurately measured or monitored.

Although both horizontal and vertical crustal deformations are prevalent in California, the present analysis is confined to the vertical deformations only—the type that are mostly human-induced (Figs. 5—7). Analysis of uneven horizontal deformation of CSP heliostat fields can be a topic of future study.


Fig. 7: Joe Poland, USGS scientist shows subsidence from 1925 and 1977 10 miles southwest of Mendota, CA. Sign reads "San Joaquin Valley California, BM S661, Subsidence 9M, 1925-1977" (Bertoldi et al. 1991).

The diagram in figure 8 is a simple geometry illustrating a portion of the CSP technology. For a given Sun position **S**, a flat mirror **M** reflects the sunray precisely onto a water-heating tower **T**. Line **MN** is the normal to the flat mirror, $\boldsymbol{\theta_i}$ is the angle of incidence for the sunray, and $\boldsymbol{\theta_{trk}}$ is the tracking angle at which the sunray is precisely reflected onto the tower **T**. For the diagram, assume a three dimensional analytic geometry of the plane connecting the Sun position, the mirror point and the tower point.

Using a hypothesis, uneven deformation will cause relative change in height of magnitude $\Delta \boldsymbol{h}$, for a given mirror in the field of heliostats (Fig. 9). Assume that this change in height will cause the mirror to move to a new position **M'**, relative to the tower position. In that case, the reflected sunray will be off target if mirror at position **M'** is in the same orientation as its previous orientation at position **M**. So, by how much should the mirror at position **M'** be rotated in order to keep reflected sunray on target at point **T** (Fig. 10)?

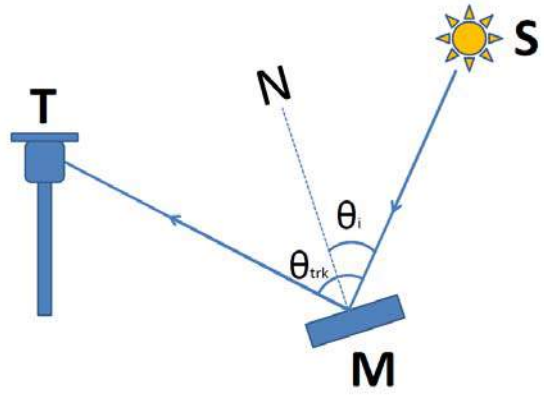


Fig. 8: Sunray tracking geometry of a flat mirror in the CSP concept

For geometrical analysis, we introduce figure 11 in which $\Delta\theta = \theta_1 - \theta_2$ is the angle by which the mirror orientation at position **M'** should be rotated to keep the reflected sunlight focused on the water-heating tower. Since the distance **MS** from the sun to the mirror is very large compared to **MT** and **M'T**, we can generally introduce a point **P** in the direction of the Sun such that the two lines **MP** and **M'P** will be parallel.

Using vector geometry, angles $\theta_1$ and $\theta_2$ in figure 11 are given by:

$$\cos(\theta_1) = \frac{\mathrm{MP} \bullet \mathrm{MT}}{|\mathrm{MP}||\mathrm{MT}|} \text{ and } \cos(\theta_2) = \frac{\mathrm{MP} \bullet \mathrm{M'T}}{|\mathrm{MP}||\mathrm{M'T}|}$$

From which we can also define direction cosines for the line vectors as follows:

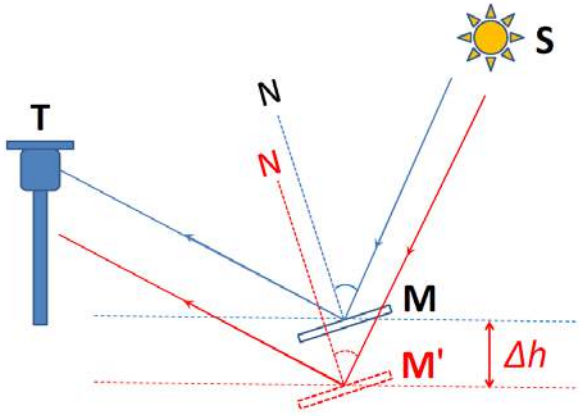


Fig. 9: Flat mirror sunray tracking geometry. A relative shift in ground height of $\Delta \boldsymbol{h}$ causes sunray reflected by **M'** to be off target. Mirror at **M** has same orientation as that of mirror at **M'**.

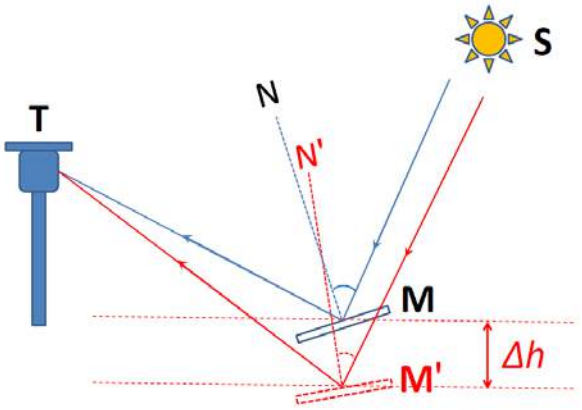


Fig. 10: Flat mirror sunray tracking geometry. Mirror at position **M'** is slightly rotated to keep reflected sun ray on target at point **T**.

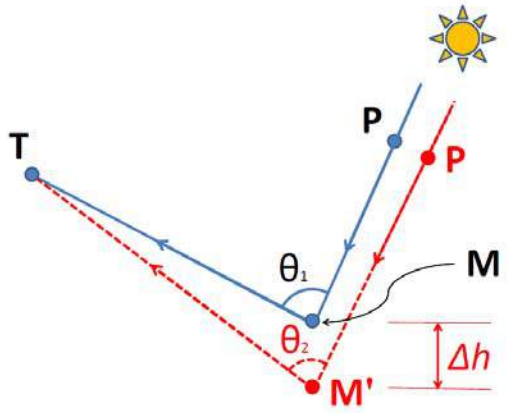


Fig. 11: Flat mirror sunray tracking geometry used in numerical analysis

$$\cos(\theta_1) = l_1 l_2 + m_1 m_2 + n_1 n_2$$
$$\cos(\theta_2) = l_1 l_3 + m_1 m_3 + n_1 n_3 \qquad (1)$$

where

$$l_1 = \cos\alpha_1, m_1 = \cos\beta_1, n_1 = \cos\gamma_1$$
$$l_2 = \cos\alpha_2, m_2 = \cos\beta_2, n_2 = \cos\gamma_2 \qquad (2)$$
$$l_3 = \cos\alpha_3, m_3 = \cos\beta_3, n_3 = \cos\gamma_3$$

$(l_1, m_1, n_1)$, $(l_2, m_2, n_2)$, $(l_3, m_3, n_3)$ are the direction cosines of **MP**, **MT**, **M'T** respectively; and $(\alpha_1, \beta_1, \gamma_1)$, $(\alpha_2, \beta_2, \gamma_2)$, $(\alpha_3, \beta_3, \gamma_3)$ are the angles which lines **MP**, **MT**, and **M'T** respectively make with the x, y, z axes.

The direction cosines in equation (2) are computed from Cartesian coordinates such as in WGS84. For example, if the line vector **MP** has a scalar distance, $\rho_{MP}$, its direction cosines are computed as follows:

$$l_1 = \frac{(X_P - X_M)}{\rho_{MP}}$$
$$m_1 = \frac{(Y_P - Y_M)}{\rho_{MP}} \qquad (3)$$
$$n_1 = \frac{(Z_P - Z_M)}{\rho_{MP}}$$

The lines **MT** and **M'T** are computed in a similar manner.

To be able to compute angles $\theta_1$ and $\theta_2$ in equation (1), the Cartesian coordinates of all the points **P**, **M**, **M'** and **T** should be known precisely. The coordinates of **M** and **T** should be known by some means (for example, from as-built surveys). The direction of the sun (elevation and azimuth) can also generally be determined at a particular instant in time. From these initial conditions, the Cartesian coordinates of **M'** and **P** can be determined as follows.

I. A relative change in ground height due to land subsidence or uplift causes point **M** to move to a new position **M'**. Therefore if **M** has ellipsoidal coordinates $(\varphi, \lambda, h)$, a change in height of magnitude $\Delta h$ will cause **M'** to have ellipsoidal coordinates $(\varphi, \lambda, h + \Delta h)$. The Cartesian coordinates of **M'** will then be:

$$X'_M = (N + h + \Delta h)\cos\varphi\cos\lambda$$
$$Y'_M = (N + h + \Delta h)\cos\varphi\sin\lambda \qquad (4)$$
$$Z'_M = \left(\left(1 - e^2\right)N + h + \Delta h\right)\sin\varphi$$

where $N = \dfrac{a}{\sqrt{1 - e^2\sin^2\varphi}}$ and $e^2 = 2f - f^2$.

The parameters $a$, $e$, and $f$ respectively refer to the Earth's semi-major axis, eccentricity and flattening.

II. Point **P** is in the direction of the sun. Therefore if the position of the sun can be known in the same coordinate system as the other points, the coordinates of **P** can be placed in the line connecting the sun and point **M**, at some distance away from **M**. Other methods can be applied—for example, a satellite in the direction of the sun. The coordinates of all the points can be determined in WGS84 system so that point **P** could be a GPS satellite in the direction of the sun. In that case, we only

need to know the azimuth and elevation of the GPS satellite at a particular instant in time. The coordinates of point **P** will then be the Cartesian WGS84 Coordinates of the satellite—roughly 20,000 km away from **M**.

## 5. NUMERICAL ILLUSTRATION

Assume three points **M**, **T**, and **P** with WGS84 coordinates as shown in Table 1.

**TABLE 1: WGS-84 GEODETIC COORDINATES**

| POINT | LATITUDE ° | LONGITUDE ° | HEIGHT m |
|---|---|---|---|
| **M** | 33.35723989 | –116.85954677 | 1662 |
| **T** | 33.35779545 | –116.85954677 | 1712 |
| **P** | 33.35640656 | –116.85954677 | 1762 |

All the three points are placed on the same geodetic plane as shown in figure 12. The initial sun direction is south of **M** and **T** is north of **M** (as may be the case for a location in Southern California). From the given coordinates,

1. **P** is roughly 100 m (arc distance) south of **M**—this translates to ≈3 arc seconds in latitude difference. **P** is 100 m higher than **M** in ellipsoidal height.
2. **T** is ≈ 60 m (arc distance) north of **M** (≈2 arc seconds in latitude difference), and is ≈50 m (150 ft.) higher than **M** in ellipsoidal height.

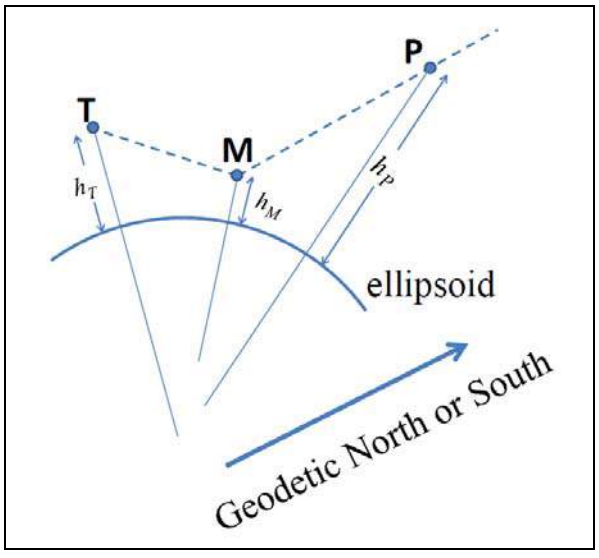


Fig. 12: Geodetic plan view of sunray tracking geometry. All the three points are in the same geodetic plane (i.e., same longitude or meridian).

Three approaches are applied to investigate the effect of Δh on **Δθ**: i) **Δθ** is computed for different angles of incidence of sunray (by varying the initial latitude angle of point **P**); ii) **Δθ** is computed for different subsidence magnitudes (i.e., for different Δh values), and iii) **Δθ** is computed for varying ellipsoidal distance of **T** from **M**.

In the first approach, the geometry is such that point **P** in the direction of the Sun is simulated at different angles of incidence ($\boldsymbol{\theta_i}$) so that the effects of crustal deformation (Δh) are computed at varying positions of the Sun. The results from this simulation indicate that crustal deformation effect (**Δθ**) is not dependent on the sunray angle of incidence ($\boldsymbol{\theta_i}$). In the second approach, a linear relationship is found between **Δθ** and Δh. However, in the third approach, **Δθ** seem to have a nonlinear quadratic relationship with the distance of the Tower from the reflecting mirror (Fig. 13)—i.e., the further away the tower **T** is from the mirror **M**, the smaller the crustal deformation effect on the tracking angle.

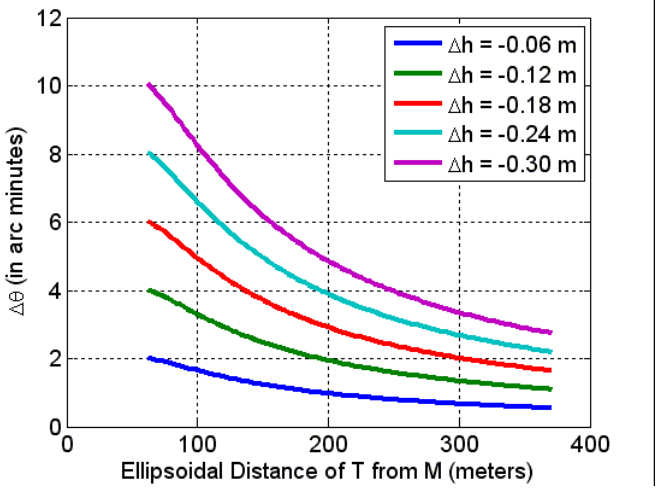


Fig. 13: Δθ versus ellipsoidal distance between **T** and **M**

## 6. SUMMARY AND CONCLUSION

This paper investigates the potential impact of crustal deformation on the CSP technology for clean electricity generation. Since the technology is only in its very early stages, to the author's best knowledge there is no existing program of continuous on-site monitoring of such hazards. Based on the tested methodology, the findings of this paper indicate that uneven (relative) crustal deformation of magnitudes starting from as small as 0.06 m may cause the geometry of sunray reflection to be off target—thus potentially compromising a CSP project. Although the current findings are solely based on geometrical analysis with simulated data, it is intended that this study may form a

basis for future research with actual field data. Furthermore, it is probably desirable to gain a better mathematical insight into a parabolic field of CSP tracking mirrors.

## 7. REFERENCES


1. Bertoldi, G.L., Johnston, R.H., and Evenson, K.D., "Ground water in the Central Valley, California"—a summary report: USGS Professional Paper 1401-A, 44 p., 1991
2. Ge, L., Ng, A. H-M., Wang, H., and Rizos, C., "Crustal deformation in Australia measured by satellite radar interferometry using ALOS/PALSAR imagery", *Journal of Applied Geodesy*, Vol. 3, Issue 1, 47–53, doi: 10.1515/JAG.2009.005, 2009
3. Hackl, M., Malservisi, R., and Wdowinski, S., "Strain rate patterns from dense GPS networks", *Natural Hazards and Earth System Sciences*, 9, 1177-1187, 2009.
4. USGS, "Monitoring ground deformation from space", USGS Fact Sheet 2005-3025, 2005.
5. Watson, K.M., Bock, Y., Sandwell, D.T., "Satellite interferometric observations of displacements associated with seasonal groundwater in the Los Angeles Basin". *J Geophys Res* 107, doi: 10.1029/2001JB000470, 2002.